Controlling the capture dynamics of traveling wave packets into a quantum dot

D. Reiter, M. Glanemann, V. M. Axt, and T. Kuhn
Institut für Festkörpertheorie, Westfälische Wilhelms-Universität Münster, Wilhelm-Klemm-Strasse 10, 48149 Münster, Germany
(Received 28 November 2005; revised manuscript received 16 February 2006; published 24 March 2006; corrected 10 May 2006)

An analysis of the control of capture processes from a traveling wave packet in a semiconductor quantum wire into localized states of a quantum dot is presented. On ultrafast time scales this capture in general leads to occupations of the discrete states as well as to coherences among these states. We show that both occupations and coherences can be efficiently controlled by excitation with a pair of spatially localized laser pulses which are spatially, temporally, or spectrally displaced with respect to each other. The coherences between discrete dot states are controlled by spatially nonoverlapping pulses by varying either their spatial or their temporal displacement. For spatially overlapping pulses an effective pulse shaping occurs which modifies both occupations and coherences. By using two-color laser pulses the dot states can be selectively addressed which may result in particularly pronounced coherences.

DOI: 10.1103/PhysRevB.73.125334 PACS number(s): 78.67.−n, 73.63.−b, 72.20.Jv, 72.10.Di

I. INTRODUCTION

Controlling a process of any kind and size has always been a principal task to physics. Such a control is particularly challenging if the process to be controlled occurs on a microscopic level. Here the dynamics is governed by quantum mechanics and one usually has only a limited access to the system via some external fields or parameters. Recently some powerful tools have been developed to control the quantum dynamics in very different systems based on the general technique of coherent control. Coherent control relies on the fact that quantum mechanical states do not only have an amplitude but also a phase which can be addressed by suitable external excitations. Due to quantum mechanical interferences this phase information can then also couple back to the amplitudes and, thus, to occupation probabilities. Coherent control techniques have previously been developed to control the outcome of chemical reactions.[1–3] In recent years they have been applied to a wide variety of phenomena in semiconductor physics including the coherent control of terahertz emission from quantum wells,[4–6] exciton and spin densities,[7,8] heavy-light hole and phonon quantum beats,[7,9–11] charge and spin currents,[12–14] light absorption,[15] quantum states in a quantum dot,[16,17] and the pure dephasing due to acoustic phonons in quantum dot structures.[18,19]

The subject of this paper is the control of a specific type of quantum dynamics, the transition of carriers in a nanostructured sample from delocalized continuum states into localized discrete states. Such transitions between states of different dimensionality are abundant in modern nanostructured devices and systems where they often provide a key ingredient for their functionality as, for example, in quantum well or quantum dot semiconductor laser. Because of their importance for heterostructure semiconductor lasers capture rates obtained from Fermi's golden rule have been calculated for many years, first mainly for the capture into quantum well states[20–24] and more recently also for the capture into quantum dot states.[25–28] Only recently the limitations of such a semiclassical treatment based on Fermi's golden rule have been overcome by using a quantum kinetic approach[29–32] which accounts for quantum coherences during the scattering process as well as the fundamental quantum mechanical uncertainties. Such quantum phenomena are of particular importance on ultrashort length and time scales.[33] In our study we are particularly interested in the combination of transport and capture processes, i.e., we assume that the carriers are generated in the continuum states in a region which is spatially separated from the localized states. They then move toward the region with the localized states where they either may be captured by means of the emission of phonons or they leave this region again after being reflected or transmitted.

To be specific we will analyze a structure where a quantum dot is embedded in a quantum wire. Such kinds of structures have already been fabricated, e.g., by cleaved edge overgrowth[34] where a dot forms at the intersection of T-shaped quantum wires or as zigzag quantum wires on a patterned substrate where dot states show up at the corners.[35] For such a structure we have recently shown that the capture dynamics when studied on ultrashort length and time scales involve a series of genuine quantum features.[32] Even at low temperatures where only phonon emission processes are possible the occupation of the bound states does not rise monotonically with time as would be expected if the capture were described by a simple capture rate. The reason is the buildup of phonon Rabi oscillations between the localized state with a phonon emitted and the delocalized state without phonon. Furthermore, in general the capture does not only lead to certain occupations of the bound states but coherent superpositions of these states may show up which then lead to a nontrivial spatiotemporal dynamics of the bound carrier density. These phenomena can only be obtained if the dynamics is treated on the quantum kinetic level which treats on the same quantum mechanical footing both transport and capture processes. Furthermore, coherences between discrete dot states are generated in wave packet transport only when the wave packet is sufficiently strongly localized in space.[30] Thus by using excitations that are ultrashort simultaneously in space and time a regime is reached where the quantum nature of the processes becomes visible.

In Ref. 32 we have studied the capture dynamics of a wave packet generated on a nanometer scale with a femto-

second laser pulse. Such localized, ultrafast excitations can be achieved by exciting the system through the tip of an optical near-field microscope.[36,37] Recently spatial resolutions smaller than 10 nm have been realized experimentally by using near-field techniques.[38–40] The basic idea of the present paper is to replace this single pulse excitation by an excitation with two pulses where we either vary the spatial separation of these pulses or the time delay between these pulses. An additional flexibility is gained if we furthermore allow the pulses to have different central frequencies corresponding to different excess energies above the band gap. We will show that in all cases an efficient control of the quantum mechanical details of the capture dynamics becomes possible.

When the pulses are focused on the same spot we recover a typical coherent control scenario: The first pulse generates an interband polarization and the second pulse interacts with the polarization created by the first pulse. This interference leads to a shaping of the effective pulse spectra and therefore modifies the generation process. If the pulses are spatially separated, on the other hand, no direct interference occurs and the phases of the pulses are of minor importance. In this case the spatial and temporal delays of the wave packets generated by the pulses become the quantities which are of central importance. The capture of the first wave packet induces coherences in the trapped carrier dynamics. The phase of these coherences at the time when the second wave packet arrives at the dot then gives rise to the control of the dynamics. We are thus dealing with a control by transport phenomena. In the most general case we have a combination of both control mechanisms, the control by spectrally shaping the exciting pulses and by the wave packet transport. By using different scenarios in combination with different quantum dot structures involving one, two, or three bound states we will analyze in detail the different control mechanisms as well as their combined action.

The paper is organized as follows: In Sec. II we briefly summarize the basic idea of the theoretical approach. In Sec. III we present numerical results for different control scenarios. After introducing the model system and discussing the general scenario of the two-pulse excitation we show how to control the coherences between the quantum dot states by using spatially separated pulses. Then we will consider the control of both occupations and coherences by using pulse shaping techniques. Finally, we show results for excitation with two-color pulses which will allow us to selectively address specific states and coherences. In Sec. IV we summarize our results and draw some conclusions.

II. THEORY

The calculations are based on the density matrix approach to quantum kinetics.[41] Starting point is a two-band model for a semiconductor including spatially inhomogeneous single-particle potentials both for electrons and holes.[42] In particular we consider a semiconductor quantum wire with an embedded quantum dot. In the lateral direction we assume infinitely high potential barriers while in the longitudinal direction the quantum dot is modeled by a potential $V^{e/h}(z) = -V_0^{e/h}\mathrm{sech}(z/a)$ for electrons and holes, respectively. Here, $V_0^{e/h}$ describes the depth of the electron/hole potential and a is a measure for the width of the dot. We take $V_0^h = \frac{2}{3}V_0^e$. This potential is only weakly reflecting and therefore allows us to concentrate on the capture process.[32] Besides the single-particle potential the model includes the coupling to an external laser field with arbitrary space and time dependence treated in the usual dipole and rotating-wave approximations. Note that the spatial variation of the laser pulses creates an effective potential for the electronic motion and thus may lead to light forces[43,44] which are fully taken into account by our theory. In our model we disregard the band degeneracies. Thus our calculation applies to a situation with fixed polarizations of all light fields. In addition our theory comprises the coupling to bulklike longitudinal optical phonons (LO phonons) via the Fröhlich interaction, and the Coulomb interaction which is treated on the mean field level. Thus, excitonic effects and the Coulomb enhancement/suppression of optical transitions are included. Details of the model can be found in Refs. 32 and 42.

The basic dynamical variables in the density matrix approach to quantum kinetics are the single-particle density matrices. In contrast to a semiclassical treatment involving transition rates the quantum kinetic formulation is independent of the choice of the single-particle basis which, therefore, may be chosen according to its convenience for numerical calculations. As has been discussed in Ref. 32, for the case of excitations sufficiently close to the band gap a representation in terms of eigenstates of the single-particle potentials is most favorable. In this representation the single-particle density matrices are defined as

$$\rho^e_{n',n} = \langle c^\dagger_{n'} c_n \rangle, \rho^h_{n',n} = \langle d^\dagger_{n'} d_n \rangle, p_{n',n} = \langle d_{n'} c_n \rangle, \tag{1}$$

where $c^\dagger_n$ and $d^\dagger_n$ (c_n and d_n) describe the creation (annihilation) of an electron and a hole in the nth eigenstate. The occupations of the single-particle states are given by the diagonal elements of the density matrix $\rho_{n,n}$ and the coherences between these states by the off-diagonal elements $\rho_{n',n}$ ($n \neq n'$). Typically, in our case the lowest few values of n refer to the discrete bound states in the quantum dot while the higher values describe quasi-continuous states in the quantum wire.

Due to the many body nature of the problem, here caused by the electron-phonon interaction, the equations of motion for the single particle density matrices lead to an infinite hierarchy of equations. In this paper the hierarchy is truncated on the level of the quantum kinetic second Born approximation. The corresponding equations of motions can be found in Ref. 42.

III. RESULTS

The general theory has been applied to a quantum dot embedded in a GaAs cylindrical quantum wire with 100 nm^2 cross section. The material parameters used in the simulations are summarized in Table I. The semiconductor quantum wire is excited with ultrashort laser pulses which are Gaussian in time and space and are modeled by a classical electric

TABLE I. Material parameters for GaAs-based structures (m_0 is the free electron mass).

Effective mass of an electron:	0.067 m_0
Effective mass of a hole:	0.45 m_0
Energy of a LO phonon:	36.4 meV
Band gap energy:	1519 meV
Static dielectric constant:	12.91
Optical dielectric constant:	10.94

field. Results for the case of excitation by a single, spatially localized pulse in the vicinity of the quantum dot have been discussed in Ref. 32. Here we extend these studies by considering a pair of such laser pulses $j=1,2$ characterized by the time of the pulse maxima t_j, the amplitudes $\mathbf{E}_j$, the position of excitations z_j, and the frequencies $\omega_j=(\epsilon_{\text{gap}}+\Delta E_j)/\hbar$, ΔE_j denoting the corresponding excess energies above the band gap ϵ_{gap} of the quantum wire. The pulse durations τ and the spatial widths σ_z are assumed to be the same for both pulses. Then, the positive frequency component of the light field is given by

$$\mathbf{E}^{(+)}(z,t)=\sum_{j=1}^{2}\mathbf{E}_j\exp\left[-\frac{(t-t_j)^2}{\tau^2}-\frac{(z-z_j)^2}{2\sigma_z^2}-i\omega_j t\right]. \quad (2)$$

The time delay between the pulses is thus given by $\Delta t=t_2-t_1$. Because of rather low excitation conditions taken in our calculations it is justified to treat the phonon system as a bath. We will restrict ourselves to the case of low temperatures where essentially only phonon emission processes occur and phonon absorption processes are negligible.

The general scenario for all our calculations is as follows: The carriers are excited above the band gap in the quantum wire outside the region of the dot. The generated wave packets, which include both positive and negative wave vector components, then split into two parts. The part with the wave vectors not directed toward the dot moves away from the quantum dot and is therefore of no interest for the capture process while the other part moves toward the quantum dot. For excess energies lower than the LO phonon energy there is no phonon emission possible as long as the wave packets are in the wire region. However, when the carriers reach the region of the dot, they can efficiently interact with phonons resulting in transitions to the bound states of the dot by emitting a phonon. As has been discussed in detail in Ref. 32 this capture results in general in a nonmonotonically rising occupation of the bound states even at low temperatures which reflects the presence of phonon Rabi oscillations. Furthermore, depending on the excitation conditions and the parameters of the quantum dot spatiotemporal oscillations inside the dot may occur demonstrating the capture into coherent superpositions of the localized states. In the following sections we will discuss different scenarios to control the occupations and/or the coherences which are based on two-pulse excitations. We will mainly focus on the behavior of the electron density matrices because, as has been shown in Ref. 32 the holes move much slower and therefore for the present excitation conditions they show no interesting features on the ultrafast time scales studied here.

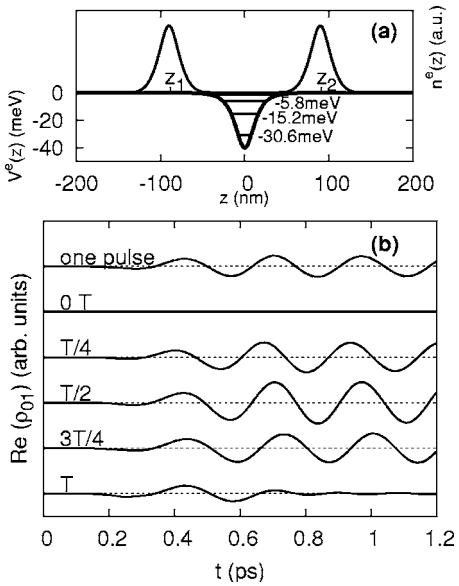

FIG. 1. (a) Electron density at $t=0$ as generated by the two laser pulses at positions $z_1=-z_2=-90$ nm for $\Delta t=0$ (top part) and quantum dot potential profile including the three bound states with their corresponding binding energies (lower part). (b) Real part of the coherences ρ_{01} between the ground and first excited state in the dot potential as a function of time for the case of excitation by 50 fs laser pulses at $z_1=-90$ nm and $z_2=90$ nm. Top curve: excitation only by one pulse at z_1 at the time $t=0$. Other curves: excitation by two pulses; the maximum of the pulse at z_1 is at $t=0$, the maximum of the pulse at z_2 at the delay time given in the figure in units of the oscillation period $T=270$ fs. The imaginary part exhibits a similar behavior and is therefore not shown.

A. Control by time delay and spatial displacement

Let us first consider the case where the two pulses have no spatial overlap. In particular we will study the case where one pulse excites a wave packet on the left side of the dot while the other acts on the right side. We consider a quantum dot with the values $V_0^e=40$ meV and $a=10$ nm, so that the quantum dot has three bound levels at the energies -30.6, -15.2, and -5.8 meV [see Fig. 1(a)]. The laser pulses have an excess energy of $\Delta E=20$ meV and a duration of $\tau=50$ fs corresponding to a full width at half maximum (FWHM) of the field amplitude of approximately 83 fs. The position of each pulse is described by its starting position $z_{1/2}$ and the variance is $\sigma_z=10$ nm corresponding to a FWHM of the amplitude of about 24 nm. At the time $t=0$ the laser pulse located at $z=z_1$ has maximum amplitude. The field amplitude is chosen rather low so that the occupations and coherences exhibit their leading order scaling with the field amplitudes.

If we excite only one packet on the left side located at $z_1=-90$ nm it splits and the parts move in both directions. The part moving toward the dot needs approximately 0.15 ps to reach the region of the dot. There it interacts with the phonons and some part of the wave packet is captured inside

the dot. In addition the packet initiates spatial oscillations inside the dot. The strength of these oscillations is related to the amplitude of the coherences. The coherence between the ground state and the first excited state ρ_{01} generated by the single pulse excitation is shown in Fig. 1(b) (top curve). We find an almost undamped oscillation starting immediately after the wave packet reaches the dot. The period of this oscillation is $T=270$ fs corresponding to the energy difference of 15.4 meV between the two states. This result which has been discussed in detail in Ref. 32 will now serve as a reference for the results of the two-pulse calculations.

Let us now add a second laser pulse with the same properties but located at the same distance on the other side of the dot, i.e., at $z_2=90$ nm. Because of the spatial separation the pulses cannot interfere so that the relative phases of the two laser pulses are irrelevant in this scenario. This second pulse has a time delay with respect to the first pulse given by Δt. Because of the spatial separation the wave packets do not interact when they are generated. The potential and the generated electron density profile at $t=0$ for the case of $\Delta t=0$ are shown in Fig. 1(a). The resulting coherences between the ground state and the first excited state for various values of Δt given in units of $T=270$ fs are shown in Fig. 1(b). Plotted is the real part of the density matrix element ρ_{01}; the imaginary part exhibits a similar behavior and is therefore not shown. We clearly observe a strong dependence of the coherences on the time delay of the two pulses.

When the second pulse acts simultaneously ($\Delta t=0$) the system is excited completely symmetrically with respect to $z=0$. This symmetry is preserved during the evolution and thus no spatial oscillations may build up. In this case all density matrix elements between an odd and an even single-particle state remain zero, in particular also ρ_{01} as can be seen in Fig. 1(b) (second curve from the top). On the other hand, when the delay time is $T/2=135$ fs the second packet reaches the dot when the captured density induced by the first packet has completed half a period. At this time both packets are at the same side of the dot. Thus the wave packet generated by the second pulse is in phase with the oscillating packet inside the dot and therefore amplifies the oscillation. Indeed it is clearly seen in Fig. 1(b) that the amplitude of the second oscillation in this case is twice as large as the first oscillation and also twice as large as for the single pulse excitation.

When the second packet is delayed by $T/4=67.5$ fs or $3T/4=202.5$ fs the amplitude is increased by about $\sqrt{2}$ due to a relative phase of $\pm\pi/2$ between the coherences. In addition the maxima and minima of the coherences are slightly shifted. The delayed packet reaches the dot when the oscillating packet is close to the middle of the dot. If the oscillating packet is moving toward the incoming second packet the oscillation is somehow slowed down when the second packet enters the dot and the maxima of the oscillation are shifted to the left. If the oscillating packet is moving away from the incoming packet the maxima are shifted to the right.

Finally, if the time delay is one period $T=270$ fs, the coherence is essentially switched off when the second packet enters the dot. The oscillation induced by the first packet is clearly observable, but it is damped when the delayed packet arrives at the dot. Again the first packet can be imagined moving back and forth through the dot and being in the starting position when the incoming delayed packet enters the dot. At this moment we have a nearly symmetrical situation for the captured electrons as if there was no time delay and the coherence is annihilated. However, this symmetry now holds only approximately and thus some very small oscillations remain in contrast to the case of zero delay where the symmetry holds exactly.

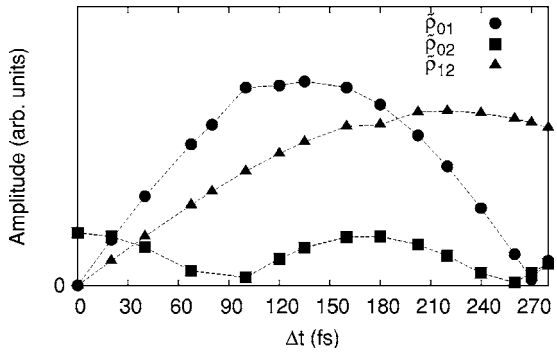

FIG. 2. Amplitude of the coherences between the three bound states in the quantum dot after the capture of both wave packets (at $t>1$ ps) as a function of the time delay between the two 50 fs laser pulses localized at $z_1=-90$ nm and $z_2=90$ nm. The lines are meant as a guide to the eye.

So far we have only discussed the coherence between ground and first excited state. In general, however, also coherences between ground and second excited states (ρ_{02}) as well as between first and second excited states (ρ_{12}) are generated by the capture process. Figure 2 shows the amplitude of these three coherences as a function of the time delay. The amplitudes have been extracted after the capture of both wave packets, i.e., at times $t>1$ ps. For ρ_{01} we recover the periodic behavior discussed above with a period of 270 fs. Also the other coherences exhibit a periodic behavior with periods determined by the respective energy differences of the states involved. We observe that, as expected, for symmetry reasons ρ_{01} and ρ_{12} vanish for $\Delta t=0$ while ρ_{02}, which describes a coherence between two even states, has a maximum in this case. Such a coherence does not lead to spatial oscillations but to a breathing behavior of the captured electron density. This is shown in Fig. 3 where we have plotted this density at three different values of the time delay in a contour plot. For $\Delta t=0$ [Fig. 3(a)] we observe a spatially symmetric electron density which is breathing with a period of 160 fs. For $\Delta t=135$ fs [Fig. 3(b)] the coherence ρ_{01} dominates leading to pronounced spatial oscillations with a period of 270 fs. In the envelope we observe a period of 440 fs resulting from ρ_{12} which is also rather strong in this case (see Fig. 2). This period is visible in the tails of the electron density because the spatial extension of the bound states increases with increasing energy of the state. For $\Delta t=270$ fs [Fig. 3(c)] essentially only ρ_{12} is nonvanishing leading to spatial oscillations with a period of 440 fs.

Instead of varying the time delay between the two laser pulses the coherence may also be controlled by varying the spatial position of the second laser pulse while both pulses are applied at the same time ($\Delta t=0$). Figure 4(a) shows the

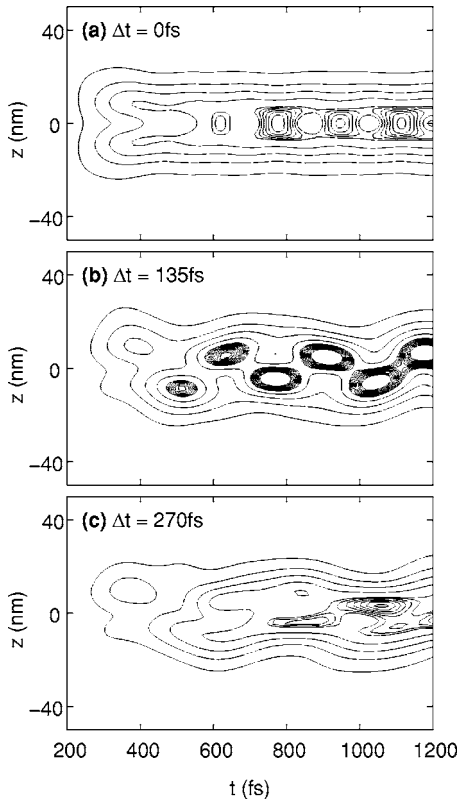

FIG. 3. Contour plot of the trapped carrier density as a function of space and time for the case of excitation by two 50 fs laser pulses at $z_1=-90$ nm and $z_2=90$ nm. The delay time between the pulses is (a) 0 fs, (b) 135 fs, and (c) 270 fs corresponding to 0, 0.5, and 1 times the oscillation period of the coherence between ground and first excited state.

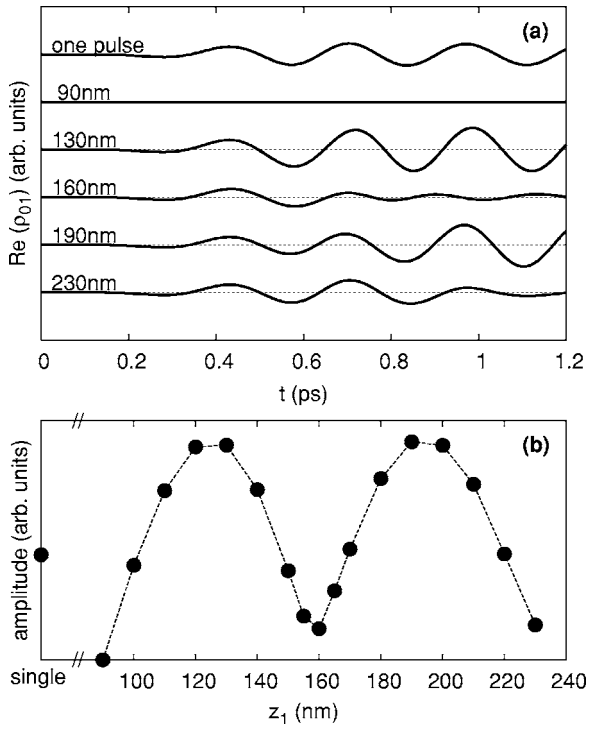

FIG. 4. (a) Real part of the coherence ρ_{01} between the ground and first excited state in the dot potential as a function of time for the case of excitation by 50 fs laser pulses with zero delay time at $z_1=-90$ nm and variable position z_2. Top curve: excitation only by one pulse at z_1. Other curves: excitation by two pulses; the position z_2 of the second pulse is as given in the figure. (b) Final amplitude of the coherence ρ_{01} (taken at $t>1$ ps) as a function of the position of the second laser pulse.

real part of the coherence ρ_{01} for this scenario where the spatial position z_2 of the right laser pulse is varied by increasing the distance to the quantum dot. The position of the left pulse is kept at $z_1=-90$ nm. The top curve again shows the reference case of a single pulse. The second curve ($z_2=90$ nm) is the completely symmetrical case discussed above where no coherence between even and odd states may build up. In the other curves now the wave packet created by the left sided pulse arrives first while the packet created by the right sided pulse arrives with some delay. Results are shown for $z_2=130$, 160, 190, and 230 nm. We again observe a periodic change between amplification and reduction of the coherence when increasing the distance of the second laser pulse from the dot. In Fig. 4(b) the amplitude of the coherence ρ_{01} is plotted as a function of the position of the right laser pulse. Obviously, the behavior is qualitatively very similar to the case of excitation with variable time delay.

However, when quantitatively analyzing the results it turns out that here some spatial transport effects come into play. Taking the group velocity of the electrons at the excess energy of the electrons, the minima in Fig. 4(b) correspond to delays in the arrival of the wave packet of about 235 and 470 fs while the maxima correspond to delays of about 120 and 350 fs. These values are similar to integer multiples of $T/2=135$ fs, which have been found above as the characteristic delay times for minima and maxima. However, they do not exactly agree with these values. The reason is that due to the dispersion in the continuum states there is a rather large broadening of the traveling wave packets before they reach the dot region (see, e.g., the spatial profiles plotted in Ref. 32) which leads to deviations from the simple estimates based only on the pulse maximum. This broadening is also responsible for the fact that the remaining coherence in the minimum is larger than in the case of excitation with temporal delay. In the case of the spatial displaced excitation the second wave packet is considerably broader when it arrives at the dot than the first one. Spatially broader wave packets, on the other hand, induce smaller coherences.[30] Therefore, the destructive interference is less perfect in this case.

The results discussed in this section have shown that coherences induced by carrier capture processes can be efficiently controlled by an excitation with two spatially separated laser pulses. As long as we remain in the low density regime, where phase space filling effects are negligible, the occupations of the quantum dot states are not changed by varying the temporal delay or spatial displacement of the laser pulses. The final occupations of the bound states in the two pulse cases studied here is always twice the value of the single pulse excitation. To control the density a different strategy has to be taken as will be discussed in the next section.

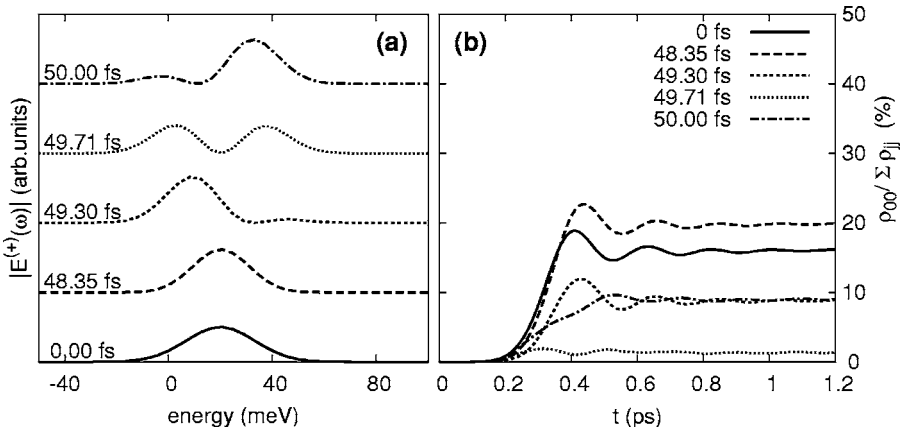

FIG. 5. (a) Shaped energy spectra normalized to the same area of the two 50 fs laser pulses which are delayed by a time Δt as given in the figure. (b) Corresponding ground state occupation of a quantum dot with one bound level at −14.4 meV as a function of time normalized to the total generated electron density.

B. Control by pulse shaping

In the cases studied in the previous section the relative phases of the two laser pulses have been irrelevant. This changes if the pulses excite the quantum wire at the same position but with a certain time delay. If there is a temporal overlap, i.e., if the delay is shorter than the pulse duration τ the pulses interfere resulting in a modified spectral distribution. Even if the delay is longer than τ but shorter than the effective dephasing time of the interband polarization such an interference is still possible giving rise to the well known coherent control phenomena.[7] Such a scenario will be the subject of the present section. Two identical pulses with the same parameters as in the previous section but with a time delay Δt excite the quantum dot at $z_1=z_2=-90$ nm. The energy spectrum of such a pulse pair is shown in Fig. 5(a) for different values of the delay. To study the influence of this pulse shaping on the capture dynamics we first consider a quantum dot with only one bound level at −14.4 meV. This dot is characterized by the values $V_0^e=30$ meV and $a=4$ nm. For this structure and pulse parameters the carriers have an excess energy approximately one LO phonon energy $\hbar\omega_{\mathrm{LO}}$ above the energy of the quantum dot state allowing for a resonant capture process.

Figure 5(b) shows the occupation of the ground state as a function of time for the delay times 0 fs (single pulse), 48.35, 49.30, 49.71, and 50.00 fs normalized to the total generated carrier density. These delay times refer to different representative scenarios reflecting the spectral characteristics as shown in Fig. 5(a). Obviously the delay time has a pronounced influence on the capture efficiency. For a time delay of $\Delta t=48.35$ fs the spectrum is narrower than the spectrum of the single pulse. Therefore the capture efficiency is with about 20% even higher than in the case of one pulse where only 18% of the generated density is captured inside the dot. We can also suppress the maximum of the spectrum by choosing a delay of $\Delta t=49.71$ fs. In this case there is no electron density generated at the resonance energy. For this reason nearly nothing is trapped in the quantum dot. A shift of the peak in the spectrum to lower or higher energies is achieved by a time delay of $\Delta t=49.30$ or 50.00 fs. Now the maximum in the energy distribution of the generated carriers is off resonant and the capture rate is lower than in the case of resonant excitation, but it does not completely vanish. Because the energy spectra are shifted almost symmetrically compared to the single pulse spectrum, the capture efficiencies for these two values of the delay are nearly equal and have a value of about 9%. By varying the time delay in fractions of a femtosecond any capture efficiency between almost 0 and 20 % can be reached. This is summarized in Fig. 6 where we have plotted the final occupation of the bound state after the traveling wave packet has passed the dot region. As is typical for an interference phenomenon, the occupation oscillates periodically with an oscillation period given by $2\pi/\omega_j$, in our case about 2.7 fs.

With the same laser pulses we now consider the quantum dot with three bound levels used in Sec. III A. By adjusting the pulse spectra we can now selectively address the capture into a specific bound state. We will see that this allows us also to gain control over the coherences between the levels. Figure 7 (left panel) shows the occupations of the three bound levels of the dot and the resulting total occupation of the bound states normalized to the total generated density as a function of time for different time delays. Here, as in the previous figures the occupations have been normalized to the total number of generated carriers. The curves therefore directly show the capture efficencies. However, it should be noted that the total number of carriers varies by about 60% when varying the time delay between the pulses. In the case of the coherences between the bound states shown in the left panel of Fig. 7 such a normalization has not been performed since here we are more interested in the total degree of coherence for varying pulse delay. As a reference the occupations and coherences for the laser pulse pair with vanishing

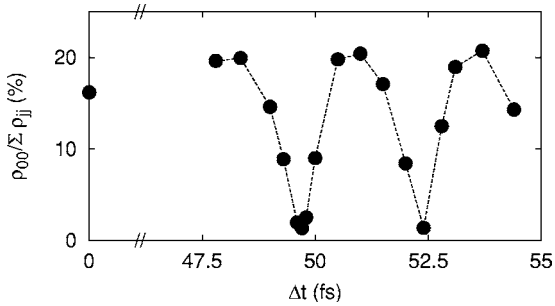

FIG. 6. Final occupation of the ground state of a dot with a single bound states after excitation with a pair of laser pulses at $z_1=-90$ nm as a function of the time delay normalized to the total generated electron density.

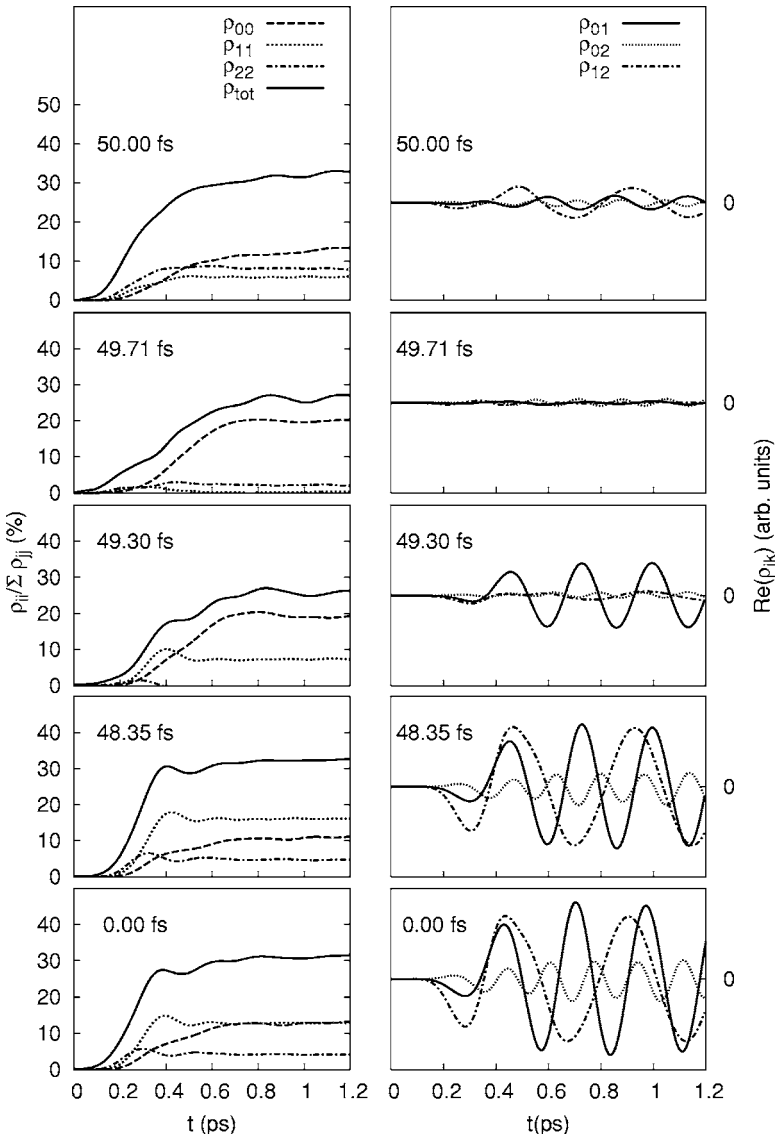

FIG. 7. Left panel: Occupation of the ground state (ρ_{00}), the first (ρ_{11}), and second (ρ_{22}) excited state, as well as the total occupation of the three bound states (ρ_{tot}) as a function of time for a quantum dot with three bound states after excitation with a pair of laser pulses at $z_1=-90$ nm for the time delays given in the figure. Right panel: Real part of the corresponding coherences (ρ_{01}, ρ_{02}, and ρ_{12}) between the bound states.

time delay are also shown. In this case the spectrum is the same as that of a single pulse and we call it unshaped. Because delay zero corresponds to maximally constructive interference the total intensity of the shaped pulses is always lower than the intensity of the unshaped pulse. For the time delays the same values as above have been taken, therefore the spectra are the same as in Fig. 5(a). Keeping in mind that the highest capture efficiencies are given by a resonant pulse whose energy is approximately one LO phonon energy above the energy of the quantum dot state we will expect that pulses with lower peak energies will mainly populate the ground state while pulses with higher peak energies will mainly populate the excited states.

Indeed the narrower pulse with a time delay of $\Delta t = 48.35$ fs increases the occupation of the first excited state of the quantum dot ρ_{11} because the pulse energy is nearly in resonance with this state while the occupations of the other levels remain nearly the same as in the case of the unshaped pulses. The coherences remain also nearly the same as in the case of unshaped pulses. For a time delay of $\Delta t = 49.30$ fs the higher energies are not excited and the occupation of the second excited state ρ_{22} is completely suppressed due to the low excitation energy. Accordingly there is no coherence between the ground level or the first excited level and the second excited level. Only the coherence between the ground state and the first excited state ρ_{01} remains. When the excitation at the maximum of the single pulse spectrum is suppressed by choosing pulses with a time delay of $\Delta t = 49.71$ fs the occupation of the first excited state ρ_{11} becomes negligibly consistent with the results above. The occupation of the second excited level ρ_{22} is suppressed as well. Simply because there is nearly no occupation in the excited states and only the ground state is populated no strong coherences can build up either. By suppressing lower energies and allowing higher energies with a time delay of $\Delta t = 50.00$ fs the occupation of the second excited state ρ_{22} is increased while the occupations of the first excited state ρ_{11} stays below ρ_{22}. The final occupations of both excited states turn out to have a similar value and consequently the coherence between the excited state ρ_{12} is higher than the coherences with the ground states ρ_{01} and ρ_{02}.

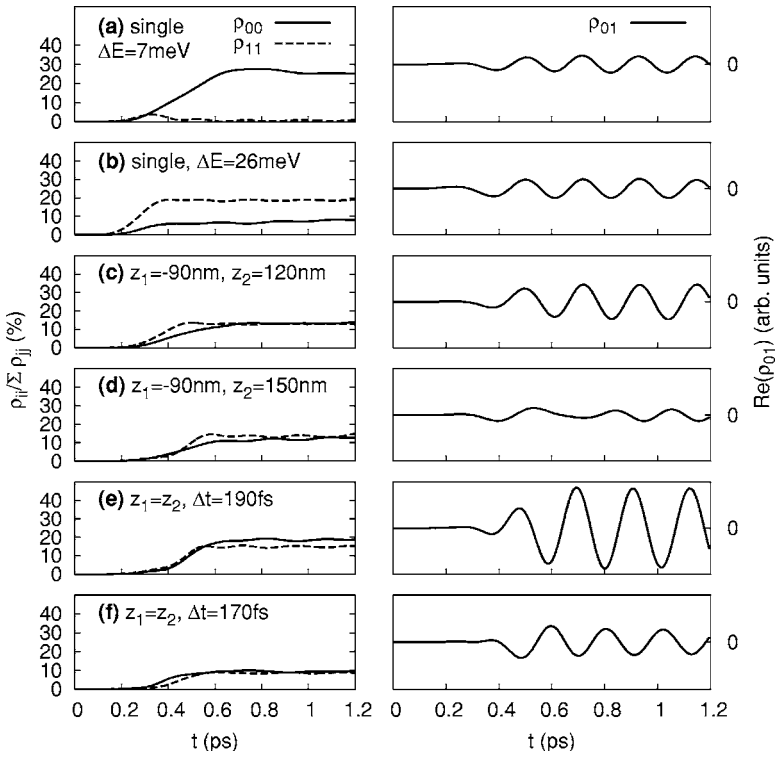

FIG. 8. Occupations of the ground state ρ_{00} and the first excited state ρ_{11} normalized to the total density (left panel) and real part of the corresponding coherence between the ground and first excited state ρ_{01} (right panel) as functions of time for a quantum dot with two bound states for the following cases: (a) single laser pulse with an excess energy of 7 meV, (b) single laser pulse with an excess energy of 26 meV, (c) and (d) combination of both laser pulses located at both sides of the dot with different distances, (e) and (f) combination of both laser pulses at the same position with different time delays.

C. Control by two-color pulses

Even more flexibility is achieved if we allow the pulses to have different excess energies, i.e., in the case of excitation by two-color pulses. In this third and last scenario we consider two pulses with different excess energies which are adjusted such that each pulse excites selectively in resonance for capture into one of the bound states of a two level dot. Here we take a dot potential with the parameters $V_0^e = 43$ meV and $a=7$ nm giving rise to bound states at the energies -30.1 and -10.5 meV. The excitation energies of the pulses are tuned one LO phonon energy above these bound states. In order to get a sharper energy distribution we take longer pulses with a pulse duration of $\tau=80$ fs (FWHM ≈ 133 fs). With spectrally sharper pulses we cannot only address selectively the occupations, but also the coherences are reduced when increasing the pulse length. A pulse with an excess energy of $\Delta E=7$ meV is used to excite the ground state. The resulting occupations and coherence of a single pulse with this excess energy can be seen in Fig. 8(a). We find that essentially only the ground state ρ_{00} is occupied and we get a moderate coherence. To excite the first excited state of the dot a laser pulse with an excess energy of $\Delta E = 26$ meV is taken. Its energy is too low to allow for two phonon processes. For a single pulse with this excess energy the occupation of the first excited state ρ_{11} is considerable higher than the occupation of the ground state ρ_{00} and the coherence is as moderate as in the case of the low energy single pulse [Fig. 8(b)]. Intending higher coherences in the following we now apply both laser pulses to the quantum wire. In order to obtain nearly equal occupations of the bound states, the amplitude of the laser pulse with the excess energy of 26 meV has been taken to be a factor of 1.5 larger than the amplitude of the pulse with the lower excess energy.

Different control mechanisms are examined and presented in Fig. 8. If we locate the two laser pulses at both sides of the dot and displace their starting position we obtain results similar to Sec. III A. Two examples for the low energy packet starting at $z_1=-90$ nm and the high energy packet at the opposite site at $z_2=120$ and 150 nm are shown in Figs. 8(c) and 8(d) taken from a series of results where the distance of the packet with higher energy was varied in steps of 10 nm from $z_2=90$ nm up to $z_2=200$ nm. The occupations are nearly the same at about 13% for all conditions [Figs. 8(c) and 8(d) left panel]. But the coherence varies with increasing distance from the dot similar to the results discussed in Sec. III A. In Fig. 8(c) (right panel) a maximum of the coherence is obtained by placing the wave packet with the higher energy at $z_2=120$ nm. The amplitude of the coherence is about twice as high as in the single pulse case. This indicates that the coherences are essentially simply added. In contrast a minimum is shown in Fig. 8(d) (right hand figure) where the right wave packet starts at $z_2=150$ nm. However, the minimum is not as pronounced as the minima obtained in Sec. III A and the oscillation is not completely suppressed when the second wave packet arrives. The reason is that now the wave packets arriving from the left and right side are different leading after the capture also to somewhat different wave packets inside the dot which cannot completely compensate each other.

If we now put both lasers on the same side of the dot we find that we can get very high coherences. Now both pulses start from the same spot $z_1=z_2=-90$ nm and we control the coherence by varying the time delay between the pulses. In the figure we show two examples where the pulse with higher energy was delayed by $\Delta t=190$ fs [Fig. 8(e)] and by $\Delta t=170$ fs [Fig. 8(f)]. When both packets start at the same side we have a mixture of pulse shaping and selective ad-

dressing. Though the excess energies of the pulses are different, they interfere and the energy spectra are shaped. The spectral selectivity resulting from the pulse shaping modifies the occupation of the discrete dot states and influences the coherence. In Fig. 8(e) the delay was adjusted to obtain a maximum of coherence. We find that the amplitude of the coherence is about six times higher than the amplitude of the coherence caused by a single laser pulse. Such a high amplitude cannot be reached when the two pulses are located at different sides of the dot. In Fig. 8(f) the delay was set to obtain a minimum of the coherence. Still the amplitude of the coherence is higher than the amplitude of the coherence induced by a single pulse. Thus, though the coherence can be controlled in this case it cannot be completely suppressed. This is a consequence of the selective excitation of the two dot states.

IV. CONCLUSIONS

As has been shown recently, capture processes from delocalized into localized states when studied on ultrashort length and time scales exhibit pronounced quantum features which cannot be described in terms of semiclassical capture rates. An oscillatory contribution in the occupation of the bound states is a signature of phonon Rabi oscillations and in the presence of more than one bound state coherent superpositions of these states may be populated resulting in a nontrivial spatiotemporal dynamics of the trapped carriers.[32] This genuine quantum mechanical behavior opens a variety of new possibilities to interact with the system and control the capture dynamics. In this paper we have shown various strategies which allowed us to efficiently control both the capture efficiency and the coherences among the localized states. All scenarios are based on the excitation with a pair of spatially localized femtosecond pulses. We employ a combination of two different control mechanisms to achieve a strong flexibility. One mechanism is of the well-known coherent control type, i.e., it is based on the relative phases of the light pulses which leads to a spectral shaping of the carrier distributions. This mechanism requires spatially overlapping pulses. The other mechanism which also works for spatially nonoverlapping pulses is a control by transport. Here the relative phases which are necessary to control the coherences of the trapped carriers result from the spatial or temporal delay of wave packets. In this case, the control is triggered by the arrival times of the wave packets at the dot.

In our first scenario two wave packets have been generated on both sides of a quantum dot and the coherence of the trapped carriers was controlled either by varying the time delay between the two pulses or by displacing the excitation position of one of the pulses. Amplification up to twice the value of the coherence induced by a single pulse was obtained. In the same way coherences which have been generated by the wave packet which arrived first at the dot could be switched off and essentially completely suppressed. In this scenario the phases of the light pulses were completely irrelevant. We thus have a pure control by transport.

In the second scenario the two laser pulses have been applied on the same side of the dot at the same position so that the pulses could interfere either directly or the second pulse could interfere with the interband polarization generated by the first one. This is a typical coherent control scenario, here, however, extended to the case of strongly inhomogeneous excitations. Due to the interference the pulse spectra are shaped depending on the time delay between the two pulses. By selecting the excitation energy we were able to control the final occupation of the discrete dot states. Typical for a coherent control phenomenon, the final occupation oscillates with the time delay, the period given by the optical period of the exciting pulses. Controlling the occupations of the dot states resulted also in a control of the coherences because a coherence between two states requires that both states have a certain occupation. We have shown that it is possible to either suppress all coherences or only a few of them.

In the third scenario we have used two-color pulses for the optical excitation. By suitably choosing the excess energies each of the pulses could be tuned such that the generated carriers are captured in essentially only one of the quantum dot states. By varying the arrival times of the wave packets generated by the two pulses very strong coherences could be achieved. In this scenario we use therefore a combination of spectral shaping of the excitation and control by wave packet transport giving rise to a large flexibility in the selection of the desired spatiotemporal dynamics of charge carriers in nanostructured samples.

In conclusion, when the excitation conditions involve simultaneously utrashort length and time scales such that a regime is reached where the quantum nature of matter is revealed, an efficient and selective control of the capture dynamics and the resulting final quantum state is feasible.

ACKNOWLEDGMENT

This work has been partially supported by the Deutsche Forschungsgemeinschaft.

[1] M. Shapiro and P. Brumer, J. Chem. Phys. **84**, 4103 (1986).
[2] M. Shapiro and P. Brumer, J. Chem. Soc., Faraday Trans. **93**, 1263 (1997).
[3] G. Vogt, G. Krampert, P. Niklaus, P. Nuernberger, and G. Gerber, Phys. Rev. Lett. **94**, 068305 (2005).
[4] I. Brener, P. C. M. Planken, M. C. Nuss, L. Pfeiffer, D. E. Leaird, and A. M. Weiner, Appl. Phys. Lett. **63**, 2213 (1993).
[5] M. S. C. Luo, S. L. Chuang, P. C. M. Planken, I. Brener, and M. C. Nuss, Phys. Rev. B **48**, 11043 (1993).
[6] W. Pötz, Appl. Phys. Lett. **72**, 3002 (1998).
[7] A. P. Heberle, J. J. Baumberg, and K. Köhler, Phys. Rev. Lett. **75**, 2598 (1995).

[8] A. P. Heberle, J. J. Baumberg, E. Binder, T. Kuhn, K. Köhler, and K. H. Ploog, IEEE J. Sel. Top. Quantum Electron. **2**, 769 (1996).
[9] T. Kuhn, V. M. Axt, M. Herbst, and E. Binder, in *Coherent Control in Atoms, Molecules, and Semiconductors*, edited by W. Pötz and W. A. Schroeder (Kluwer Academic Publishers, Dordrecht, 1999), p. 113.
[10] M. U. Wehner, M. H. Ulm, D. S. Chemla, and M. Wegener, Phys. Rev. Lett. **80**, 1992 (1998).
[11] V. M. Axt, M. Herbst, and T. Kuhn, Superlattices Microstruct. **26**, 117 (1999).
[12] A. Haché, J. E. Sipe, and H. M. van Driel, IEEE J. Quantum Electron. **34**, 1144 (1998).
[13] R. D. R. Bhat, P. Nemec, Y. Kerachian, H. M. van Driel, J. E. Sipe, and A. L. Smirl, Phys. Rev. B **71**, 035209 (2005).
[14] R. D. R. Bhat and J. Sipe, Phys. Rev. Lett. **85**, 5432 (2000).
[15] W. Pötz, Phys. Rev. Lett. **79**, 3262 (1997).
[16] N. H. Bonadeo, J. Erland, D. Gammon, D. Park, D. S. Katzer, and D. G. Steel, Science **282**, 1473 (1998).
[17] P. Chen, C. Piermarocchi, L. J. Sham, D. Gammon, and D. G. Steel, Phys. Rev. B **69**, 075320 (2004).
[18] U. Hohenester and G. Stadler, Phys. Rev. Lett. **92**, 196801 (2004).
[19] V. M. Axt, P. Machnikowski, and T. Kuhn, Phys. Rev. B **71**, 155305 (2005).
[20] H. Shichijo, R. M. Kolbas, N. Holonyak, R. D. Dupuis, and P. D. Dapkus, Solid State Commun. **27**, 1029 (1978).
[21] J. A. Brum and G. Bastard, Phys. Rev. B **33**, 1420 (1986).
[22] T. Kuhn and G. Mahler, Solid-State Electron. **32**, 1851 (1989).
[23] P. W. M. Blom, C. Smit, J. E. M. Haverkort, and J. H. Wolter, Phys. Rev. B **47**, 2072 (1993).
[24] M. Preisel and J. Mørk, J. Appl. Phys. **76**, 1691 (1994).
[25] R. Ferreira and G. Bastard, Appl. Phys. Lett. **74**, 2818 (1999).
[26] I. Magnusdottir, S. Bischoff, A. V. Uskov, and J. Mørk, Phys. Rev. B **67**, 205326 (2003).
[27] A. Markus and A. Fiore, Phys. Status Solidi A **201**, 338 (2004).
[28] T. R. Nielsen, P. Gartner, and F. Jahnke, Phys. Rev. B **69**, 235314 (2004).
[29] T. Kuhn, M. Glanemann, and V. M. Axt, Physica B **314**, 455 (2002).
[30] M. Glanemann, V. M. Axt, and T. Kuhn, Phys. Status Solidi C **0**, 1523 (2003).
[31] J. Seebeck, T. R. Nielsen, P. Gartner, and F. Jahnke, Phys. Rev. B **71**, 125327 (2005).
[32] M. Glanemann, V. M. Axt, and T. Kuhn, Phys. Rev. B **72**, 045354 (2005).
[33] V. M. Axt and T. Kuhn, Rep. Prog. Phys. **67**, 433 (2004).
[34] W. Wegscheider, G. Schedelbeck, G. Abstreiter, M. Rother, and M. Bichler, Phys. Rev. Lett. **79**, 1917 (1997).
[35] C. Lienau, V. Emiliani, T. Guenther, F. Intonti, T. Elsaesser, R. Nötzel, and K. H. Ploog, Phys. Status Solidi A **178**, 471 (2000).
[36] V. Emiliani, T. Guenther, C. Lienau, R. Nötzel, and K. H. Ploog, Phys. Rev. B **61**, R10583 (2000).
[37] T. Guenther, C. Lienau, T. Elsaesser, M. Glanemann, V. M. Axt, T. Kuhn, S. Eshlaghi, and A. D. Wieck, Phys. Rev. Lett. **89**, 057401 (2002).
[38] R. Hillenbrand, Science **100**, 421 (2004).
[39] J. M. Gerton, L. A. Wade, G. A. Lessard, Z. Ma, and S. R. Quake, Phys. Rev. Lett. **93**, 180801 (2004).
[40] Y. C. Martin and H. K. Wickramashinghe, J. Appl. Phys. **91**, 3363 (2001).
[41] F. Rossi and T. Kuhn, Rev. Mod. Phys. **74**, 895 (2002).
[42] M. Herbst, M. Glanemann, V. M. Axt, and T. Kuhn, Phys. Rev. B **67**, 195305 (2003).
[43] M. Lindberg and R. Binder, J. Phys.: Condens. Matter **15**, 1119 (2003).
[44] R. Binder and M. Lindberg, J. Phys.: Condens. Matter **18**, 729 (2006).